

## 1 Response Surface Methodology for Oxidative Degradation of the 2 Basic Yellow 28 Dye by Temperature and Ferrous Ion Activated Persulfate

3 BELGIN GÖZMEN<sup>1,\*</sup>, ÖZGÜR SÖNMEZ<sup>1</sup> and MERAL TURABIK<sup>2</sup>

4 <sup>1</sup>Department of Chemistry, Faculty of Science & Arts, Mersin University, Yenisehir, Mersin 33343, Turkey

5 <sup>2</sup>Chemical Prog., Technical Science Vocational School, Mersin University, Yenisehir, Mersin 33343, Turkey

6 \*Corresponding author: Fax: +90 324 3610046; Tel: +90 324 3610001; E-mail: bgozmen@mersin.edu.tr

(Received: ;

Accepted: )

AJC-0000

7 The decomposition of the persulfate by Fe<sup>2+</sup> ions results in the production of oxidative sulfate radical anions. In present study, the  
8 oxidative degradation of the basic yellow 28 dye solution was studied by using persulfate and ferrous ions. To obtain maximum mineralization  
9 efficiency for aqueous solution of basic yellow 28, Box-Behnken design combined with response surface modeling (RSM). Four independent  
10 variables, namely temperature (40-70 °C), initial concentration of persulfate (4-12 mM), ferrous ion (1-3 mM) and time (2-8 h) were  
11 transformed to coded values. Subsequently, it was determined that quadratic model to be the most suitable models to estimate the responses.  
12 Analysis of variance (ANOVA) was carried out for quadratic model and was observed the significance of the independent variables and  
13 their interactions. The predicted values of the oxidative degradation efficiency were verified to be in good agreement with the experimental  
14 values (R<sup>2</sup> = 0.9902 and R<sup>2</sup><sub>adj</sub> = 0.9804). Maximum mineralization efficiency 93 % was obtained under following conditions: persulfate  
15 concentration 9.87 mM, ferrous ion concentration 1.95 mM, temperature at 65 °C and time at 8 h for 40 mg/L basic yellow 28 aqueous  
16 solution.

17 **Key Words: Oxidative degradation, Green chemistry, Basic yellow 28, Persulfate, Response surface methodology, Box-Behnken design.**

### INTRODUCTION

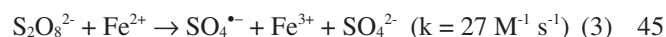
18 During the dye production and textile manufacturing  
19 processes, large volumes of dyeing wastewater which has the  
20 potential of toxicity and intense colour has been left into aquatic  
21 systems. Even if dye concentrations were low values (e.g.,  
22 10-20 mg L<sup>-1</sup>), it affects the water transparency and solubility  
23 of gases in water. Besides, the cationic dyes are generally  
24 considered to be more toxic in comparison to the anionic dyes  
25 toward the aquatic biota<sup>1</sup>. This is because cationic dyes easily  
26 interact with the membrane surfaces of the negatively charged  
27 cells, enters into the cells and concentrates in the cytoplasm<sup>2</sup>.  
28 Subsequently, the symbiotic process is affected as the natural  
29 equilibrium is disturbed by the reduced photosynthetic activity.  
30 The above mentioned reduction in the photosynthetic activity  
31 is due to the colouration of the water in the streams.

32 In recent years, there has been growing interest in the use  
33 of persulfate (S<sub>2</sub>O<sub>8</sub><sup>2-</sup>), which is one of the strongest oxidants  
34 known in aqueous solutions<sup>3-5</sup>. It offers certain advantages over  
35 other oxidants, such as high stability at room temperature, high  
36 aqueous solubility, a solid fact that can be easily stored and  
37 transferred and relatively low cost<sup>6,7</sup>. Persulfate anion with  
38 a redox potential of 2.01 V is a non-selective oxidant. This

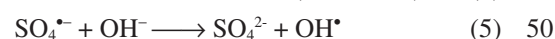
oxidant can be decomposed by heat, UV light or transition  
metal ions (Me<sup>n+</sup>), such as Fe<sup>2+</sup>. Subsequently, this leads to the  
formation of SO<sub>4</sub><sup>•-</sup>, which exhibits a redox potential of 2.6 V<sup>8,9</sup>.



If a ferrous ion is used as the transition metal: 44



In a persulfate-water system, hydroxyl radicals can also  
be formed, as shown in eqns. 4-5. The hydroxyl radicals may  
participate in the oxidation of the contaminants<sup>10</sup>. 48



Response surface methods (RSM) offer statistical design  
of experiment tools that lead to peak process performance.  
The RSM-based modeling studies have been widely used in  
many wastewater treatment systems such as photocatalytic  
oxidation<sup>11</sup>, Fenton/photo-Fenton<sup>12,13</sup>, electro-Fenton/photo-  
electron-Fenton<sup>14,15</sup>, electrochemical oxidation<sup>16</sup>, ozonation<sup>17</sup>,  
wet air oxidation<sup>18</sup> and adsorption<sup>19,20</sup> for various pollutants.  
To our best of knowledge, optimization of oxidative degradation 58

59 process parameters of persulfate/iron/temperature system to  
 60 obtain maximum mineralization of basic yellow 28 by using  
 61 with the Box-Behnken design has not been study conducted  
 62 until now. Many researchers had investigated the alone oxidative  
 63 effect of the heat, persulfate dosage and/or metal ions amount  
 64 on activated persulfate by temperature or metal ions for various  
 65 types of organics<sup>21-25</sup>. Anipsitakis and Dionysiou<sup>5</sup> investigated  
 66 the activation of persulfate by 9 different transition metals  
 67 including Ag<sup>+</sup>, Ce<sup>3+</sup>, Co<sup>2+</sup>, Fe<sup>2+</sup>, Fe<sup>3+</sup>, Mn<sup>2+</sup>, Ni<sup>2+</sup>, Ru<sup>3+</sup> and V<sup>3+</sup>  
 68 and reported that Ag<sup>+</sup> is the best activating agent for persulfate.  
 69 Despite this result, in environmental applications iron is often  
 70 used due to environmentally friendly nature, cost effectiveness.  
 71 However, Liang *et al.*<sup>4</sup> found that Fe<sup>2+</sup> used in small incre-  
 72 ment In previous studies have shown that an increase in pH<sup>3,5,7,25</sup>  
 73 and ionic strength<sup>3,25</sup> resulted in a decrease in the rate constant  
 74 of organic pollutants. Xu and Li<sup>7</sup> reported that the inhibiting  
 75 effects of some ions ranged from low to high in an order of  
 76 NO<sub>3</sub><sup>-</sup> < Cl<sup>-</sup> < H<sub>2</sub>PO<sub>4</sub><sup>-</sup> < HCO<sub>3</sub><sup>-</sup>. It has been known that in the  
 77 neutral and alkaline media, the amounts of soluble Fe<sup>2+</sup> and  
 78 Fe<sup>3+</sup> could decrease due to the formation of complexes and  
 79 precipitations. For this reason, the chelating agents were  
 80 employed to stabilize the iron in solution at near neutral pH or  
 81 pH of the solution was adjusted under pH 4 value. Some of  
 82 previous studies have been performed to determine the opti-  
 83 mum conditions, but in most of them one of the three variables  
 84 (temperature, persulfate concentration, Fe<sup>2+</sup> concentration)  
 85 were kept constant<sup>7,24,26</sup>. Also optimum values obtained from  
 86 these studies differ from each other.

87 In the present study, basic yellow 28 (Cationic Gold  
 88 Yellow X-GL) which is a synthetic basic cationic dye, imparts  
 89 a yellow colour in the aqueous solution, was selected as the  
 90 target dye. A series of experiments were conducted at ambient  
 91 temperatures (between 40-70 °C) to evaluate the effectiveness  
 92 of the persulfate oxidation that activated by ferrous ion for the  
 93 destruction of basic yellow 28. The Box-Behnken design of  
 94 Design Expert® 8 program was used for the response surface  
 95 methodology in the experimental design during the first  
 96 series of experiments. The experiments were designed to  
 97 determine the influence of factors, such as temperature, initial  
 98 ferrous ion and persulfate concentrations and time on the degra-  
 99 dation as well as studying the optimum working state. The  
 100 second series of experiments were investigated for the oxida-  
 101 tive degradation pathway of basic yellow 28 at optimum  
 102 conditions.

## EXPERIMENTAL

103 **Response surface modeling:** Response surface method-  
 104 ology (RSM) uses mathematical and statistical techniques to  
 105 fit of a polynomial equation to the experimental data, which  
 106 should be the objective of making the statistical previsions<sup>27</sup>.  
 107 Determine the optimum set of operational variables for a process  
 108 is the main goal of the RSM. The statistical experimental  
 109 designing with RSM can reduce the process variability,  
 110 experimentation time as well as the overall cost with an improved  
 111 process output<sup>28</sup>. The Box-Behnken design (BBD) of Design  
 112 Expert® 8 program was used for the RSM in the experimental  
 113 design where each factor takes only three levels. This design  
 114 is more efficient and economical according to the other 3k

115 designs, especially for a large number of variables<sup>28</sup>. The  
 116 independent variables of temperature, processing time, initial  
 117 K<sub>2</sub>S<sub>2</sub>O<sub>8</sub> and initial FeSO<sub>4</sub> concentration were coded with the  
 118 low and high levels in the Box-Behnken design, as shown in  
 119 Table-1. The mineralization per cent (TOC removal%) of the  
 120 basic yellow 28 solution was the obtained response. In the  
 121 optimization process, the responses can be simply related to  
 122 the chosen factors by the linear or quadratic models. A  
 123 quadratic model is shown as follows:

$$Y = \beta_0 + \sum_{j=1}^k \beta_j x_j + \sum_{j=1}^k \beta_{jj} x_j^2 + \sum_{i < j=2}^k \beta_{ij} x_i x_j + e_i \quad (6) \quad 124$$

125 where, Y is the response, k is the number of factors, x<sub>i</sub> and x<sub>j</sub>  
 126 are the coded variables, β<sub>0</sub> is the offset term, β<sub>j</sub>, β<sub>jj</sub> and β<sub>ij</sub>  
 127 are the first-order, quadratic and interaction effects respectively, i  
 128 and j are the index numbers for factor and e<sub>i</sub> is the residual  
 129 error<sup>29</sup>.

130 Model fitting and graphical analyses were carried out  
 131 using the Design-Expert software. Soundness of the fit was  
 132 studied using F-test, p-value, chi-square (X<sup>2</sup>), the root mean  
 133 square error of prediction (RMSEP) and the relative error of  
 134 prediction (RSEP), correlation coefficient (R<sup>2</sup>) and adjusted  
 135 correlation coefficient (R<sup>2</sup><sub>adj</sub>).

136 **General procedures:** Basic yellow 28 (BY28) was  
 137 supplied by the DyStar textile firm with the commercial name  
 138 Astrazone Goldgelb GL-E. Potassium persulfate (K<sub>2</sub>S<sub>2</sub>O<sub>8</sub>) and  
 139 ferrous sulfate (FeSO<sub>4</sub>·7H<sub>2</sub>O) were obtained from Acros and  
 140 Merck, respectively. The aqueous solutions were prepared in  
 141 high purity de-ionized water (resistivity 18.2 mΩ cm), which  
 142 was obtained using a Milli-Q water purification system  
 143 (Millipore). The basic yellow 28 stock solution was prepared  
 144 at 1000 mg/L. The desired concentration (40 mg L<sup>-1</sup>) of basic  
 145 yellow 28 was obtained through the appropriate dilutions of  
 146 the stock solution. The K<sub>2</sub>S<sub>2</sub>O<sub>8</sub> and FeSO<sub>4</sub> solutions (100 mM)  
 147 were prepared prior to each batch experiment. However, the  
 148 FeSO<sub>4</sub> solution was prepared in acidic de-ionized water (pH  
 149 3.5).

150 The batch experiments for the decomposition of the basic  
 151 yellow 28 solution were carried out in plugged borosilicate  
 152 glass bottles. The initial concentration of basic yellow 28 was  
 153 prepared as 40 mg L<sup>-1</sup> from the stock solution. The pH was  
 154 adjusted to 3.5 with 0.5 M H<sub>2</sub>SO<sub>4</sub>. The reaction solutions were  
 155 obtained by adding the FeSO<sub>4</sub> solution and the K<sub>2</sub>S<sub>2</sub>O<sub>8</sub> solution  
 156 into the aqueous basic yellow 28 solutions with a total volume  
 157 of 60 mL. The mineralization experiments were conducted in  
 158 a thermo-controlled (±1 °C) water bath shaker at 120 rpm at  
 159 different temperatures (40-70 °C) in the range of 2 to 8 h. The  
 160 experiments were carried out in parallel. At the end of the  
 161 reaction time, sodium azide was added to quench any further  
 162 oxidation reactions. Subsequently, the aliquots of the samples  
 163 were withdrawn from the reactor and filtered through a 0.45  
 164 μm membrane filter before the analysis.

165 **Detection methods:** The total organic carbon (TOC)  
 166 contents of the aliquots were analyzed by using the Merck  
 167 TOC cell test (1.14878.0001 / 5.0 - 80.0 mg L<sup>-1</sup> TOC). At the  
 168 end of the reaction time, the sample aliquots were immediately  
 169 filtered through a 0.45 μm membrane. The TOC contents of  
 170 the cell tests were measured by using the Merck Spectroquant  
 171 NOVA 30 model photometer.

TABLE-1  
EXPERIMENTAL RESULTS OF BOX-BEHNKEN DESIGN EXPERIMENTS

| Run | X <sub>1</sub> : [S <sub>2</sub> O <sub>8</sub> <sup>2-</sup> ] <sub>0</sub> | X <sub>2</sub> : [Fe <sup>2+</sup> ] <sub>0</sub> | X <sub>3</sub> : T (°C) | X <sub>4</sub> : t (h) | Observed TOC removal (%) (Y) | Predicted TOC removal (%) (Y) |
|-----|--|---|-------------------------|------------------------|------------------------------|-------------------------------|
| 1   | 4 (-1)   | 1 (-1)  | 55 (0)                  | 5 (0)                  | 26                           | 21                            |
| 2   | 12 (+1)  | 1 (-1)  | 55 (0)                  | 5 (0)                  | 64                           | 65                            |
| 3   | 4 (-1)   | 3 (+1)  | 55 (0)                  | 5 (0)                  | 48                           | 47                            |
| 4   | 12 (+1)  | 3 (+1)  | 55 (0)                  | 5 (0)                  | 43                           | 47                            |
| 5   | 8 (0)  | 2 (0)   | 40 (-1)                 | 2 (-1)                 | 4                            | 3                             |
| 6   | 8 (0)  | 2 (0)   | 70 (+1)                 | 2 (-1)                 | 57                           | 54                            |
| 7   | 8 (0)  | 2 (0)   | 40 (-1)                 | 8 (+1)                 | 62                           | 65                            |
| 8   | 8 (0)  | 2 (0)   | 70 (+1)                 | 8 (+1)                 | 91                           | 91                            |
| 9   | 4 (-1)   | 2 (0)   | 55 (0)                  | 2 (-1)                 | 16                           | 16                            |
| 10  | 12 (+1)  | 2 (0)   | 55 (0)                  | 2 (-1)                 | 43                           | 40                            |
| 11  | 4 (-1)   | 2 (0)   | 55 (0)                  | 8 (+1)                 | 65                           | 68                            |
| 12  | 12 (+1)  | 2 (0)   | 55 (0)                  | 8 (+1)                 | 88                           | 88                            |
| 13  | 8 (0)  | 1 (-1)  | 40 (-1)                 | 5 (0)                  | 23                           | 25                            |
| 14  | 8 (0)  | 3 (+1)  | 40 (-1)                 | 5 (0)                  | 28                           | 27                            |
| 15  | 8 (0)  | 1 (-1)  | 70 (+1)                 | 5 (0)                  | 61                           | 62                            |
| 16  | 8 (0)  | 3 (+1)  | 70 (+1)                 | 5 (0)                  | 69                           | 67                            |
| 17  | 4 (-1)   | 2 (0)   | 40 (-1)                 | 5 (0)                  | 22                           | 22                            |
| 18  | 12 (+1)  | 2 (0)   | 40 (-1)                 | 5 (0)                  | 42                           | 40                            |
| 19  | 4 (-1)   | 2 (0)   | 70 (+1)                 | 5 (0)                  | 54                           | 57                            |
| 20  | 12 (+1)  | 2 (0)   | 70 (+1)                 | 5 (0)                  | 81                           | 82                            |
| 21  | 8 (0)  | 1 (-1)  | 55 (0)                  | 2 (-1)                 | 18                           | 22                            |
| 22  | 8 (0)  | 3 (+1)  | 55 (0)                  | 2 (-1)                 | 21                           | 24                            |
| 23  | 8 (0)  | 1 (-1)  | 55 (0)                  | 8 (+1)                 | 72                           | 70                            |
| 24  | 8 (0)  | 3 (+1)  | 55 (0)                  | 8 (+1)                 | 79                           | 76                            |
| 25  | 8 (0)  | 2 (0)   | 55 (0)                  | 5 (0)                  | 71                           | 74                            |
| 26  | 8 (0)  | 2 (0)   | 55 (0)                  | 5 (0)                  | 75                           | 74                            |
| 27  | 8 (0)  | 2 (0)   | 55 (0)                  | 5 (0)                  | 72                           | 74                            |
| 28  | 8 (0)  | 2 (0)   | 55 (0)                  | 5 (0)                  | 77                           | 74                            |
| 29  | 8 (0)  | 2 (0)   | 55 (0)                  | 5 (0)                  | 76                           | 74                            |

172 The TOC removal % was calculated according to the equa-  
173 tion given below:

$$174 \quad \text{TOC}_{\text{removal}(\%)} = \left[ \frac{\text{TOC}_0 - \text{TOC}_t}{\text{TOC}_0} \right] \times 100$$

175 where, TOC<sub>0</sub> and TOC<sub>t</sub> are the initial and final TOC (mg L<sup>-1</sup>)  
176 content values of the solution before and after the oxidative  
177 treatment, respectively.

178 For the ammonium, nitrate and nitrite analysis, 2 mL  
179 samples were taken from the reaction bottles at the different  
180 time intervals. Next, methanol (0.5 mL) was added to quench  
181 any further oxidation reactions. The DIONEX ICS 3000 Dual  
182 model ion chromatograph equipped with a conductivity detector,  
183 an AS9-HC, 4 mm × 250 mm anion-exchange and CS12A 4  
184 mm × 250 mm cation-exchange columns were used to measure  
185 the inorganic ions. The mobile phase was a solution of: sodium  
186 carbonate (10 mM) and a total flow rate of 1.0 mL/min for the  
187 anion analysis, *meta*-sulfonic acid (0.02 N) and a total flow  
188 rate of 1.0 mL/min for the cation analysis.

189 The GC-MS analysis was performed with the 5890A  
190 Agilent model gas chromatograph, interfaced with the ECD,  
191 NPD and 5975C mass selective detector. The aqueous solutions  
192 were extracted three times with 50 mL dichloromethane. A  
193 3 mL sample was analyzed on GC-MS. The analytical column,  
194 which was connected to the system, was an HP5-MS capillary  
195 column (30 m × 0.25 mm × 0.25 μm). Helium was used as the  
196 carrier gas with a flow rate of 2 mL/min. The GC injection  
197 port temperature was 250 °C (split mode = 1/5) and the column

temperature was fixed at 70 °C for 5 min. Subsequently, the  
198 column temperature was programmed from 70 to 150 °C at  
199 4 °C/min and then from 150 to 280 °C with the 5 °C/min rate.  
200 The MS detector was operated in the EI mode (70 eV).  
201

## RESULTS AND DISCUSSION

**Evaluation of experimental results with design-expert:** 202  
A set of four process variables, the operating temperature (40-  
203 70 °C), the K<sub>2</sub>S<sub>2</sub>O<sub>8</sub> initial concentration (4-12 mM), the FeSO<sub>4</sub>  
204 initial concentration (1-3 mM) and processing time (2-8 h)  
205 were identified to investigate their influences on the TOC  
206 removal % of basic yellow 28 at initial pH 3.5. These intervals  
207 were determined as a result of preliminary experiments. When  
208 the dye solutions were mixed with various ion concentrations  
209 of S<sub>2</sub>O<sub>8</sub><sup>2-</sup> and the Fe<sup>2+</sup>, the dye immediately started to degrade.  
210 The reaction intermediates can occur during the oxidation of  
211 the target compounds. It is possible that some of the interme-  
212 diate products are more toxic and long-lived than starting com-  
213 pounds during decomposition. Therefore, it is important to  
214 monitor the contents of the TOC in various stages of treatment.  
215 Mineralization of the treated basic yellow 28 solutions during  
216 the S<sub>2</sub>O<sub>8</sub><sup>2-</sup>/Fe<sup>2+</sup> oxidative treatment was followed by measuring  
217 the total organic carbon (TOC). For the above mentioned four  
218 variables, a set of 29 experiments is required (Table-1). Box-  
219 Behnken design is a spherical, revolving design. It consists of  
220 five replicates central point (C<sub>p</sub>) and the edge points are located on  
221 a hypersphere equidistant from C<sub>p</sub>. Calculate the number of necess-  
222 ary experiments number is made according to the following  
223



224 formula:  $N = 2k(k-1) + C_p$ , where  $k$  is the number of factors  
225 and  $C_p$  is the number of the central points. The experimental  
226 results obtained in the Box-Behnken design with the real and coded  
227 values for the four variables studied are shown in Table-1.

228 In an aqueous medium, the individual and interactive  
229 effects of the setted four variables on the mineralization of the  
230 basic yellow 28 dye in an aqueous medium were investigated  
231 using the Box-Behnken design application. The experimental  
232 results were evaluated with RSM of Design-Expert® 8. The  
233 approximating functions of the TOC removal percent ( $Y$ ) in  
234 terms of the coded variables obtained are shown as follows:

$$235 \quad Y = 74.20 + 10.83X_1 + 2.00X_2 + 19.33X_3 + 24.83X_4 - 10.75X_1X_2 +$$

$$1.75X_1X_3 - 1.00X_1X_4 + 0.75X_2X_3 + 1.00X_2X_4 - 6.00X_3X_4 -$$

$$12.14X_1^2 - 17.14X_2^2 - 11.89X_3^2 - 9.14X_4^2 \quad (7)$$

236 Fig. 1 provides Pareto graphic analysis, respectively. These  
237 analyses introduce single or synergistic positive or inimical  
238 effects of variables on the studied response<sup>30</sup>. Pareto graphic  
239 analysis based on the following formula gives the percentage  
240 effects of each factor on the response.

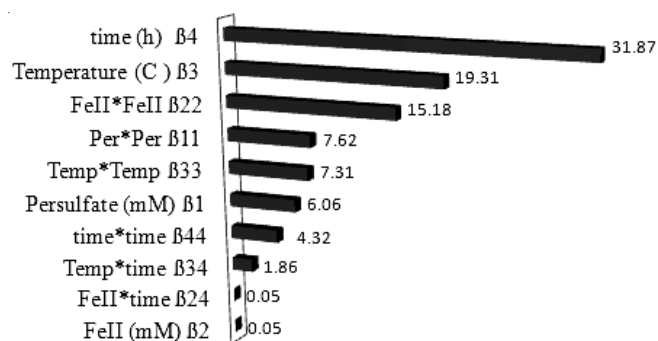


Fig. 1. Graphical pareto analysis

$$241 \quad P_i = \left( \frac{\beta_i^2}{\sum \beta_i^2} \right) \times 100 \quad (i \neq 0) \quad (8)$$

242 It is demonstrated that the processing time ( $\beta_4$ ), temper-  
243 ature ( $\beta_3$ ) and persulfate ion initial concentration ( $\beta_1$ ) are the  
244 crucial factors for the mineralization of basic yellow 28. How-  
245 ever, the ferrous ion initial concentration ( $\beta_2$ ) has a slight  
246 influence on the oxidation. Analysis of variance and regression  
247 takes place in almost all statistical studies. The relationships  
248 between an unlimited number of independent variables and a  
249 response or dependent variable are investigated by regression.  
250 Regression also allows values on one variable to be predicted  
251 from the values recorded on one or more other variables. In  
252 the same way, ANOVA places no restriction on the number of  
253 groups or conditions that may be compared, while factorial  
254 ANOVA allows examination of the influence of two or more  
255 independent variables or factors on a dependent variable with  
256 t-test statistics in the program for eqn. 6. As a result of the  
257 experimental data quadratic model was determined as statisti-  
258 cally significant. The quadratic regression model was highly  
259 significant as the F-test (F-value) was found to be 101.16  
260 with a very low probability value (P-value < 0.0001). This  
261 indicated that only 0.01 % of the model was due to noise<sup>31</sup>. If  
262 the model has a high degree of adequacy to predict of the

263 experimental results, the computed F-value should be greater  
264 than the tabulated F-value at a level of significance  $\alpha$ . There-  
265 fore, the calculated F-value ( $F_{\text{model}} = 101.16$ ) was compared  
266 with the tabulated F-value ( $F_{0.05, df, (n-(df+1))}$ ) at significance level  
267 of 0.05, when the  $df$  for model is 14 and  $n = 29$ . The Tabular  
268 F-value ( $F_{0.05, 14, 14} = 2.48$ ) is clearly less than calculated F-  
269 value<sup>20</sup>.

270 To test the fit between the model responses and the  
271 observed data is performed chi-square ( $\chi^2$ ) test. This value  
272 was computed by the following equations<sup>20</sup>:

$$\text{Chi-Square} = \sum_{i=1}^N \frac{(Y_{\text{meas},i} - Y_{\text{pred},i})^2}{Y_{\text{pred},i}} \quad (9) \quad 273$$

274 where  $Y_{\text{pred},i}$  and  $Y_{\text{meas},i}$  are the model predicted and measured  
275 values of the variable,  $Y$  and  $N$  is the number of run.

276 The calculated chi-square value of the model ( $\chi^2 = 4.60$ )  
277 was found to be less than the tabulated value ( $\chi^2_{0.05} = 41.34$ ).  
278 This result revealed that there is not a significant difference  
279 between the observed data and model response. The quality  
280 of the fit of the polynomial model was also expressed by the  
281 determination of correlation coefficient,  $R^2$  and the adjusted  
282 coefficient  $R^2_{\text{adj}}$ . The correlation between the experimental data  
283 and predicted responses is explained by the value of  $R^2$ . The  
284 obtained values of  $R^2$  and  $R^2_{\text{adj}}$  were 0.9902 and 0.9804,  
285 respectively. The adjusted  $R^2$  ( $R^2_{\text{adj}}$ ) value is more suitable to  
286 compare the models with different numbers of the independent  
287 variables.  $R$  squared estimates the proportion of the dependent  
288 variable variance that can be attributed to the predictors, but  
289 unfortunately this statistic exhibits an overestimate bias. The  
290 smaller adjusted  $R$  squared attempts to eliminate this bias<sup>32</sup>.  
291 As shown Fig. 2(a), the correlation coefficient ( $R^2$ ) between  
292 the experimental and model predicted values of the response  
293 variable showed the goodness of fit of the model. A plot of the  
294 normal probability of the residuals is shown in Fig. 2(b). The  
295 residuals from the analysis should be normally distributed.  
296 The above mentioned plot is an important diagnostic tool to  
297 detect and explain the systematic departures from the assump-  
298 tion<sup>33</sup>. The trend of the residual to a normal distribution, where  
299 the errors are normally distributed and independent of each  
300 other is shown in Fig. 2(b) In addition, the error variance is  
301 homogeneous. Signal to noise ratio is measured by "Adeq  
302 Precision" which value should be greater than 4. The ratio of  
303 35.60 indicates an adequate signal. Fig. 2(c) displays a plot of  
304 residuals *versus* predicted response that provides a handy  
305 diagnostic for nonconstant variance. In this case, the pattern  
306 exhibits the hoped-for random scatter, suggesting the variance  
307 of original observations is constant for all values of the  
308 response.

309 An effective tool for checking lurking variables that may  
310 have influenced the response during the experiment is the  
311 normal plot of the standardized residuals *versus* the experi-  
312 mental run number as shown in Fig. 2(d). The plot should  
313 show a random scatter around the center line and within the  
314 interval of  $\pm 3.50$ . Trends indicate a time-related variable  
315 lurking in the background. Blocking and randomization  
316 provide insurance against trends ruining the analysis<sup>34</sup>. As a  
317 result, Fig. 2(d) represents that there was no apparent deviation  
318 with the observation order ( $\pm 3.00$ ).

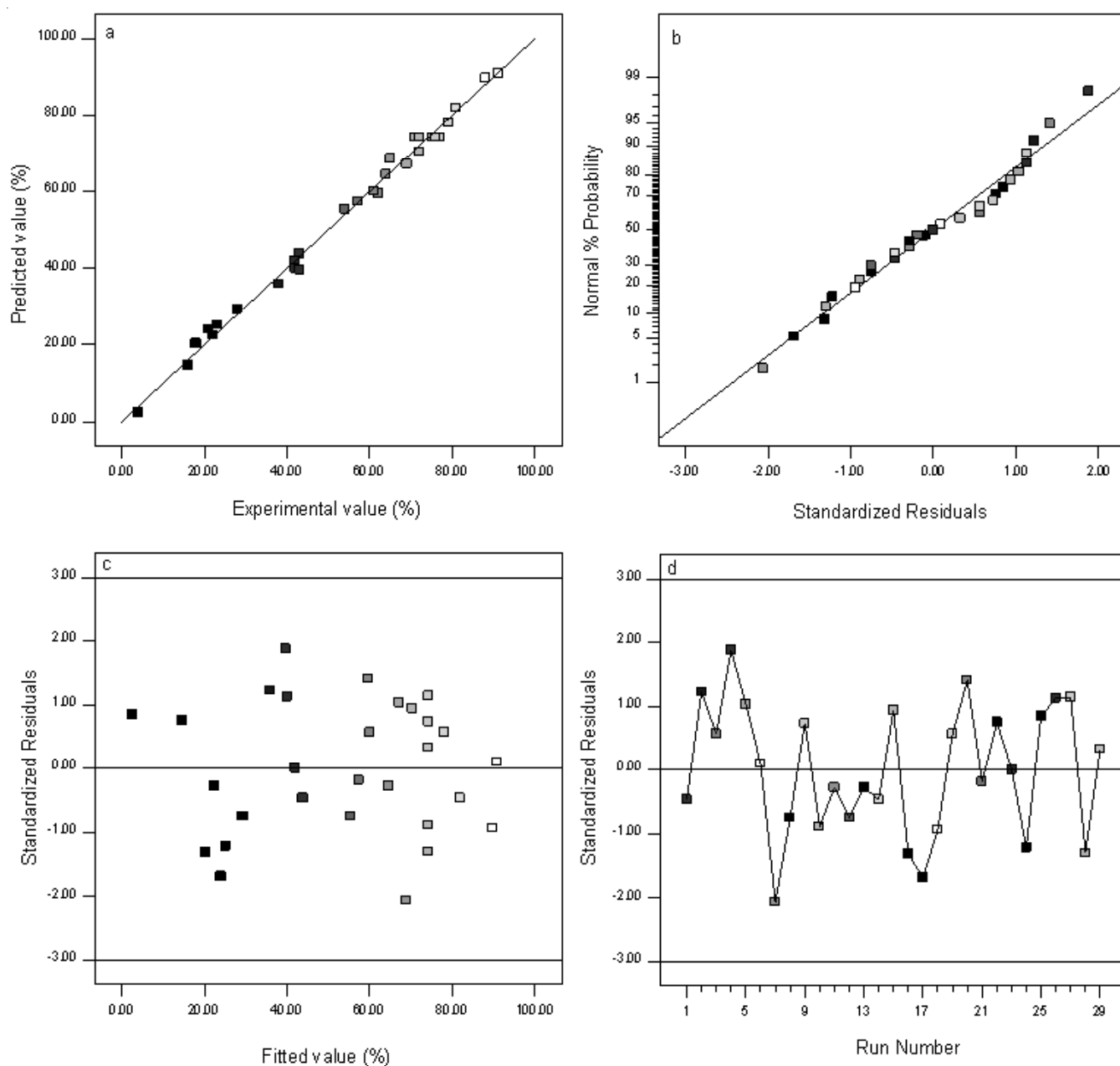


Fig. 2. (a) The actual and predicted plot of TOC removal percent ( $R^2 = 0.9902$  and  $R^2_{adj} = 0.9804$ ), (b) the standardized residual and normal % probability plot of TOC removal percent, (c) the predicted TOC removal percent and standardized residuals plot, (d) the standardized residuals plot for TOC removal efficiency

319 **Effects of variables in the three-dimensional response**  
 320 **surface plots:** The contour plot and the corresponding 3D  
 321 view for the initial persulfate ion concentration *versus* the  
 322 initial ferrous ion concentration, while holding temperature at  
 323 65 °C and time 8 h is shown in Fig. 3(a). It is well established  
 324 that persulfate plays an important role as a source of  $SO_4^{\bullet-}$   
 325 production in the  $S_2O_8^{2-}/Fe^{2+}$  oxidative treatment. In the present  
 326 study, various initial concentrations of  $S_2O_8^{2-}$  in the range of  
 327 4 and 12 mM were used for the mineralization of the basic  
 328 yellow 28 dye in an aqueous solution to obtain its optimal  
 329 concentration. The TOC removal per cent values showed fast  
 330 increase due to an increase of the initial persulfate concentra-  
 331 tion to 10 mM, especially  $Fe^{2+}$  concentration in the range  
 332 of 1.5-2.25 mM. The TOC removal percentage value reached  
 333 96 % at the end of the 8 h experiments, while the persulfate

concentration was 9.7 mM at  $[Fe^{2+}]_0 = 2$  mM. However, an  
 334 increase of the persulfate concentration beyond 10 mM  
 335 resulted in a decrease in the mineralization efficiency. Regarding  
 336 the effect of iron appears to have been achieved the best  
 337 results around 2 mM. If the concentration of  $Fe(II)$  is less than  
 338 1.5 and higher than 2.5 mM, the TOC removal percents may  
 339 decrease.  
 340

Temperature is one of the main parameters which influence  
 341 the production of  $SO_4^{\bullet-}$  in the oxidative processes based on  
 342 persulfate. In Fig. 3(b), the response surface and contour plots  
 343 show that obtained TOC removal (%) values as a function of  
 344 the initial persulfate concentration and reaction temperature,  
 345 keeping the initial concentration of  $Fe^{2+}$  at 2 mM and time at 8  
 346 h. It can clearly be observed that a rise in the temperature is  
 347 significantly effective on the removal of basic yellow 28. When  
 348

349 the effects of the temperature and persulfate concentration on  
 350 TOC removal were investigated, the effective temperature and  
 351 persulfate concentration intervals were obtained as 55-65 °C  
 352 and 8-10 mM, respectively. The effect of time and concentra-  
 353 tion of Fe(II) on the TOC removal is shown in Fig. 3(c).  
 354 The highest TOC removal data was obtained when the  
 355 concentration of Fe(II) was hold around 2 mM. Fig. 3(d) shows  
 356 the TOC removal per cent at the mentioned range of time and  
 357 temperature, keeping the initial concentration of Fe<sup>2+</sup> at 2 mM  
 358 and persulfate at 8 mM. An increase in TOC conversion with  
 359 both time and temperature was observed. This tendency can  
 360 be explained as follows: based on a previously described free-  
 361 radical involved reaction mechanism, the concentration of free  
 362 radicals increases with temperature and then enhances the  
 363 organic compounds degradation. Fig. 3(d) is examined, when  
 364 the amount of Fe(II) is kept around 2 mM, the results show  
 365 that the temperature should be adjusted over 60 °C and the  
 366 time should be over 6.5 h.

367 Oh *et al.* obtained that the rate of poly(vinyl alcohol) (PVA)  
 368 (50 mg L<sup>-1</sup>) oxidation was maximized when the persulfate to  
 369 Fe<sup>2+</sup> molar ratio was 1:1 at 20 °C (250 mg L<sup>-1</sup> K<sub>2</sub>S<sub>2</sub>O<sub>8</sub> = 0.92  
 370 mM K<sub>2</sub>S<sub>2</sub>O<sub>8</sub>)<sup>24</sup>. They also observed that increasing the temperature  
 371 from 20 to 80 °C accelerated the oxidation rate of poly(vinyl

372 alcohol), at these temperatures degradation of poly(vinyl  
 373 alcohol) was completed 120 and 30 min, respectively. But,  
 374 TOC removal of poly(vinyl alcohol) in the experiments has  
 375 not been followed. Li *et al.* also investigated the effect of pH,  
 376 persulfate concentration, ionic strength, temperature and cata-  
 377 lytic Fe<sup>3+</sup> and Ag<sup>+</sup> on the degradation efficiency of diphenyl-  
 378 amine (DPA) by persulfate in batch experiments<sup>25</sup>. They  
 379 observed that Ag<sup>+</sup> ion is more efficient than Fe<sup>3+</sup> ion and the  
 380 increase of either the pH value or ionic strength caused those  
 381 inhibitive effects on the degradation of diphenylamine (20 µg  
 382 mL<sup>-1</sup>). Their results showed that the rate of diphenylamine  
 383 degradation increased as the initial persulfate concentration  
 384 increased in the range of 4.4 to 33 mM. Nfodzoi and Choi<sup>26</sup>  
 385 has also investigated degradation of triclosan by using  
 386 persulfate/Ag<sup>+</sup> ion. They found that an oxidant: metal molar  
 387 ratio of 1:1 (stoichiometric amount) was not an optimum for  
 388 degradation of this substance. As a result, it is reported that  
 389 the reactivity of oxidant/metal systems to be depending on  
 390 the target compound. In another study<sup>7</sup>, an azo dye orange G  
 391 (OG) was degraded by the persulfate/ferrous system at pH  
 392 3.5. Batch experiments were performed in 50 mL test tubes.  
 393 In the above mentioned study it was observed that at [Fe<sup>2+</sup>] =  
 394 1 mM, increasing the dosage of persulfate from 1 to 4 mM

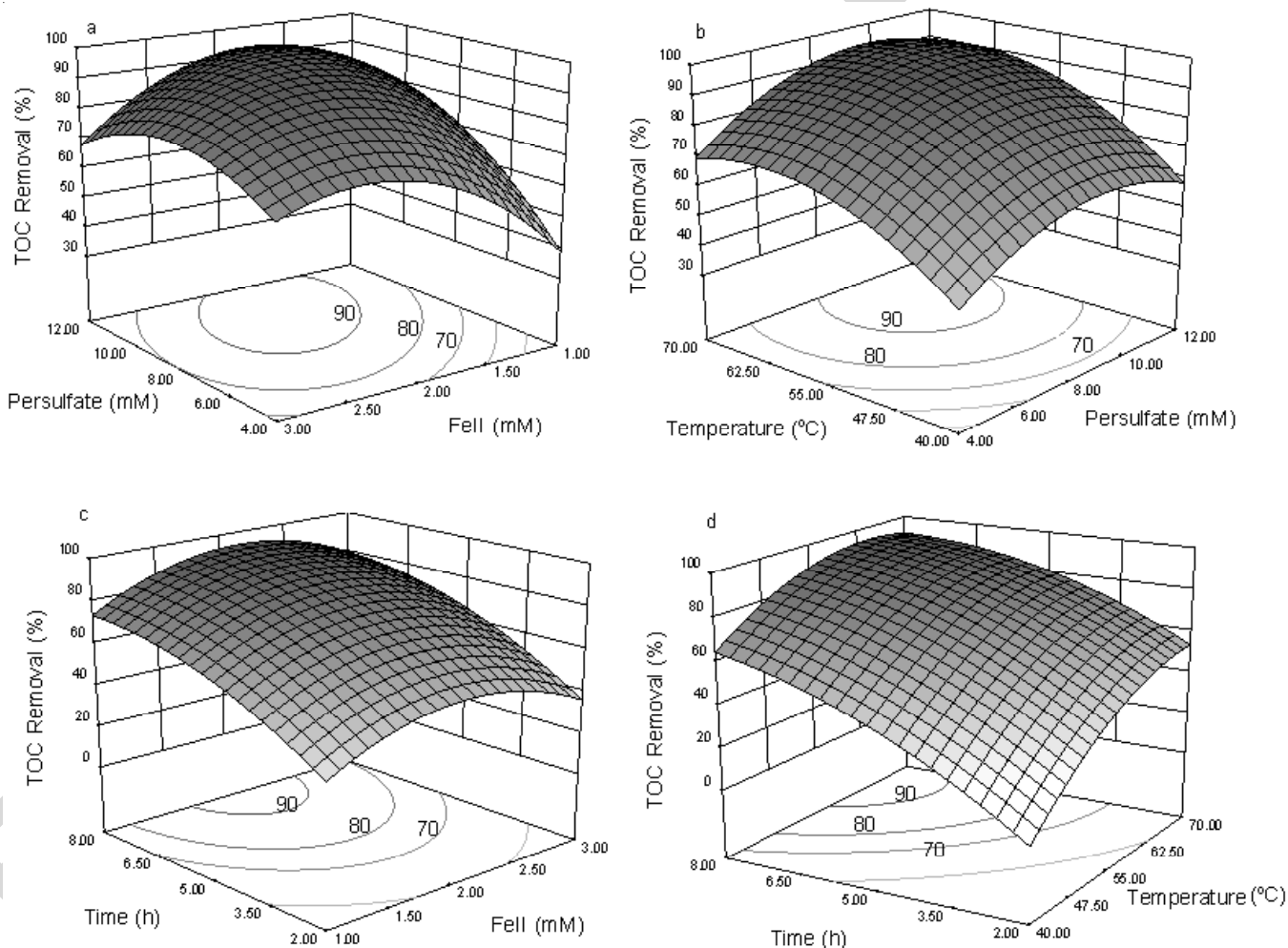
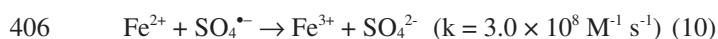
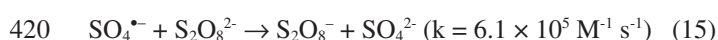
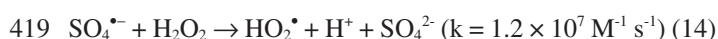
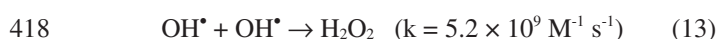


Fig. 3. The effect of (a) initial persulfate and ferrous ion concentrations ( $T = 65\text{ }^{\circ}\text{C}$ ,  $t = 8\text{ h}$ ), (b) temperature and persulfate concentration ( $[\text{Fe}^{2+}]_0 = 2\text{ mM}$ ,  $t = 8\text{ h}$ ), (c) time and ferrous ion concentrations ( $T = 65\text{ }^{\circ}\text{C}$ ,  $[\text{S}_2\text{O}_8^{2-}]_0 = 8\text{ mM}$ ), (d) time and temperature ( $[\text{Fe}^{2+}]_0 = 2\text{ mM}$ ,  $[\text{S}_2\text{O}_8^{2-}]_0 = 8\text{ mM}$ ) on TOC removal

395 ([Persulfate]/[Fe<sup>2+</sup>] = from 1:1 to 4:1) resulted in an increase  
396 orange G degradation. When Fe<sup>2+</sup> concentration varied from  
397 0.5 to 4 mM (persulfate concentration is kept constant as 4  
398 mM), the efficiency of orange G degradation was increased  
399 from 54 to 99 % within 0.5 h. In this study, the optimum condi-  
400 tions for orange G degradation was found as persulfate at 4  
401 mM and ferrous ion at 4 mM at pH 3.5 and 20 °C. However,  
402 with a further increase of the Fe<sup>2+</sup> concentration up to 8 mM,  
403 orange G degradation reduced<sup>7</sup>. The above mentioned tendency  
404 explained that the ferrous ion can also act as a sulfate radical  
405 scavenger at its high concentration, according to eqn. 10.



407 The optimum conditions obtained in the present study  
408 differs from others may be due to differences both target comp-  
409 ound and experimental conditions. In addition to the previous  
410 studies the effects of four variables alone or interaction on  
411 basic yellow 28 degradation has been examined with the RSM  
412 in the present study. The negative effect of the ferrous ion was  
413 determined over the 2.5 mM Fe(II) value. The sulfate radicals  
414 were also consumed by some other reactions<sup>35-37</sup>:



421 In work of Gozmen and Turabik, the degradation of basic  
422 yellow 28 at the same concentration was performed by UV/  
423 TiO<sub>2</sub>/IO<sub>4</sub><sup>-</sup> system and was obtained 85 % of mineralization  
424 after 3 h treatment at pH 5.2 ([IO<sub>3</sub><sup>-</sup>] = 5 mM)<sup>38</sup>. However, the  
425 obtained mineralization values of this study are lower than in  
426 the previous study. It could be said that persulfate/Fe<sup>2+</sup> system  
427 is not very effective on the degradation of basic yellow 28  
428 dye, but it can be thought of as environmentally friendly and  
429 more economical.

430 It is also established that the TOC removal decreases with  
431 the Fe<sup>3+</sup> and/or Fe<sup>2+</sup> ions in the solution because of the formation  
432 of Fe ions complexes with carboxylic acids and the degradation  
433 products<sup>39</sup>. To understand the combined effect of S<sub>2</sub>O<sub>8</sub><sup>2-</sup>/Fe<sup>2+</sup>,  
434 the experiments were conducted with the use of Fe<sup>2+</sup> and S<sub>2</sub>O<sub>8</sub><sup>2-</sup>  
435 alone. However, the TOC removal was not achieved in the  
436 above mentioned experiments.

437 **Optimization of the removal of dye:** The experimental  
438 results were optimized by Design-Expert software using the  
439 approximating function of basic yellow 28 removal percent in  
440 eqn. 7. Desirability is an objective function that ranges from  
441 zero outside of the limits to one at the goal. The simultaneous  
442 objective function is a geometric mean of all transformed  
443 responses:

$$444 \quad D = (d_1 \times d_2 \times \dots \times d_n)^{\frac{1}{n}} = \left( \prod_{i=1}^n d_i \right)^{\frac{1}{n}} \quad (11)$$

445 The d<sub>i</sub>, which ranges from 0 to 1 (the least to most desir-  
446 able, respectively), conceives the desirability of each individual

(i) response and the number of responses being optimized is 447  
n<sup>34</sup>. 448

The numerical optimization finds a point that maximizes 449  
the desirability function. The characteristics of a goal may be 450  
altered by adjusting the weight or importance. For several 451  
responses and factors, all goals get combined into one desir- 452  
ability function. The possible goals are: maximize, minimize, 453  
target, within range, none (for responses only) and set to an 454  
exact value (factors only)<sup>40</sup>. In this study, all factors was in the 455  
range of experimental design value, whereas removal of basic 456  
yellow 28 were maximized. Fig. 4 shows the TOC removal % 457  
values in the end of the maximization study for the basic yellow 458  
28 removal per cent (between 85 and 100 %) with the desir- 459  
ability value of 1 depending on the selected goal for the variables. 460  
Optimal conditions were chosen as persulfate at 9.87 mM and 461  
ferrous ion at 1.95 mM, time at 8 h and temperature at 65 °C 462  
to avoid spending excess persulfate and ferrous ions for 40 463  
mg L<sup>-1</sup> basic yellow 28 at pH 3.5. The optimal parameter values 464  
were validated through persulfate/ferrous oxidation experi- 465  
ments. As a result of confirmatory experiments are performed 466  
by using the optimal conditions and closely results (93 %) 467  
was obtained with the data from optimization analysis using 468  
desirability function. 469

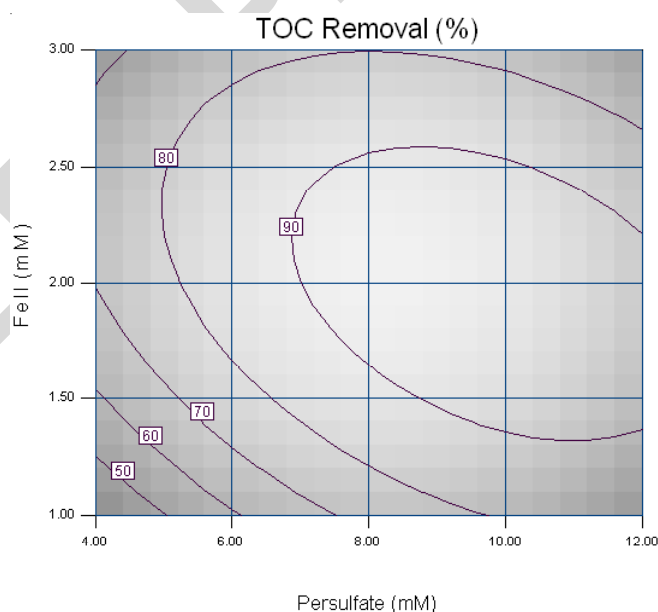


Fig. 4. The maximize TOC removal % values with desirability value of 1 (between 85 and 100 %)

**Identification of intermediates:** A solution 40 mg L<sup>-1</sup> of 470  
basic yellow 28 was treated for 20, 60, 180 and 300 min at 471  
65 °C. The remaining organics were extracted for the analysis 472  
of GC-MS. The hydroxyl radical and sulfate radical anion are 473  
powerful oxidants, which can degrade the organic molecules 474  
at a faster rate<sup>41</sup>. The degradation reaction of a dye can be 475  
written as follows: 476



The direct degradation of basic yellow 28 using S<sub>2</sub>O<sub>8</sub><sup>2-</sup> 479  
may be ignored, because of no detectable degradation was 480  
observed after 1 h treatment at room temperature. The aromatic 481



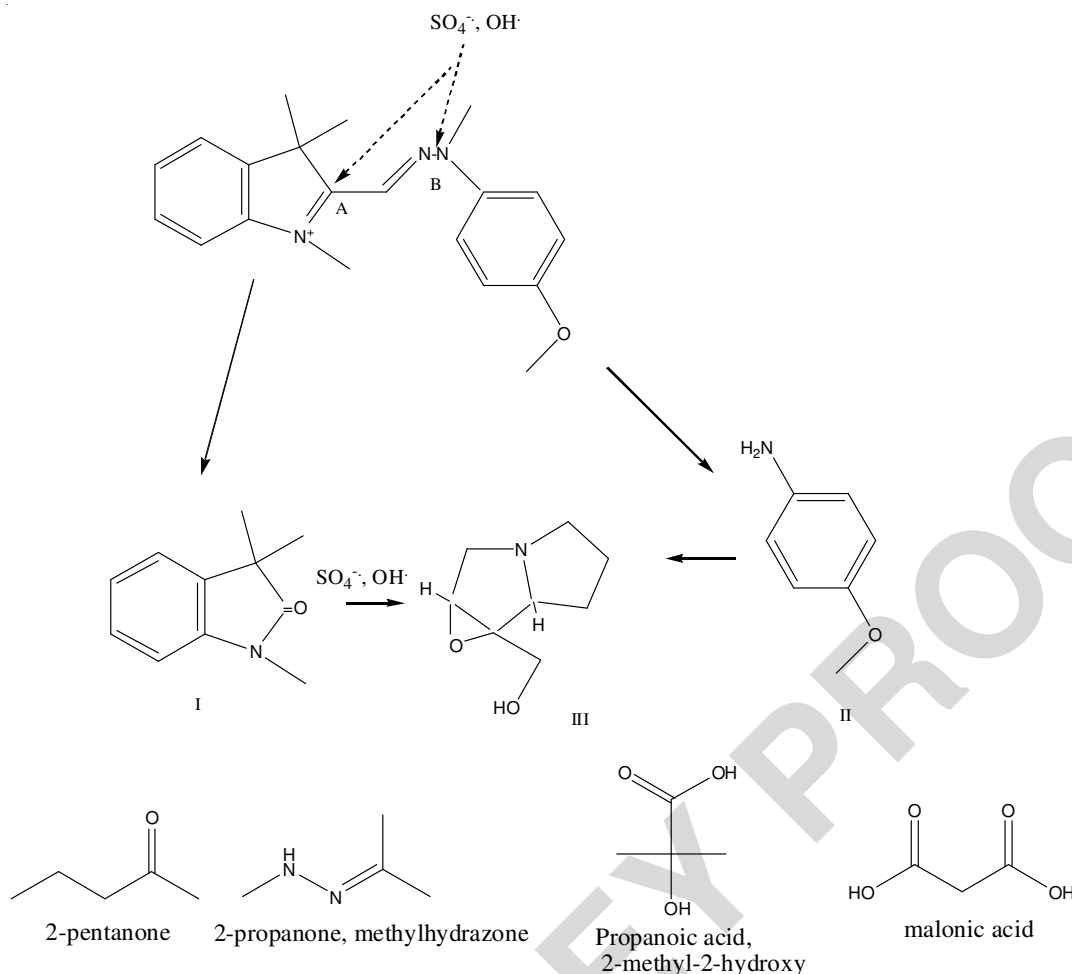


Fig. 5. Proposed reaction scheme for the initial degradation of basic yellow 28 by persulfate/ferrous oxidation

482 oxidation reaction intermediates identified at the early stage  
 483 (after 20 min for 65 °C) of the  $S_2O_8^{2-}/Fe^{2+}$  treatment may  
 484 indicate that the degradation pathway was initiated by two  
 485 possible paths. This was due to the oxidative attack of the  
 486 radicals. The probable pathway can be described by Fig. 5. As  
 487 the observed structures of I and III, it can be said that the main  
 488 attack of the radicals materialized to regions of A and B, which  
 489 contain the double bond. On the one hand, 2-indolinone 1,3,3-  
 490 trimethyl (I) comes from the hydroxyl radical attack on A re-  
 491 gion, while on the other hand benzenamine-4-methoxy (II)  
 492 comes from the cleavage of the N-N (-C=N-N) bond (B  
 493 region). The supinidine, 1-β, 2-β-epoxy (III) can form from  
 494 the hydroxylation of (I). Then, oxidative ring opening reac-  
 495 tions lead to formation of small structures such as 2-pentanone  
 496 ( $M^+$ : 86), 2-propanone, methylhydrazone ( $M^+$ : 86), 2-pentanone  
 497 ( $M^+$ : 86), malonic acid ( $M^+$ : 104) and propanoic acid, 2-  
 498 methyl-2-hydroxy ( $M^+$ : 104) (detected at before 5 min). After  
 499 the attack on the B region by the radicals, the nitrogen element  
 500 departed from the aqueous phase as  $NO_3^-$ ,  $NO_2^-$  or  $NH_4^+$ . In  
 501 the basic yellow 28 dye structure, basic yellow 28 absorbance  
 502 value at 438 nm was not observed due to the conjugated  
 503 chromophore group is broken in the oxidative degradation  
 504 process. This signifies the removal of the dye.

505 Mineralization of basic yellow 28 leads to the conversion  
 506 of the nitrogen and sulfur heteroatoms present in the molecule  
 507 into inorganic ions, such as nitrate, nitrite, ammonium and

sulfate ions. The evolution of these inorganic ions monitored 508  
 by the ion chromatography analyses at 65 °C during the 509  
 treatments is shown in Fig. 6. 510

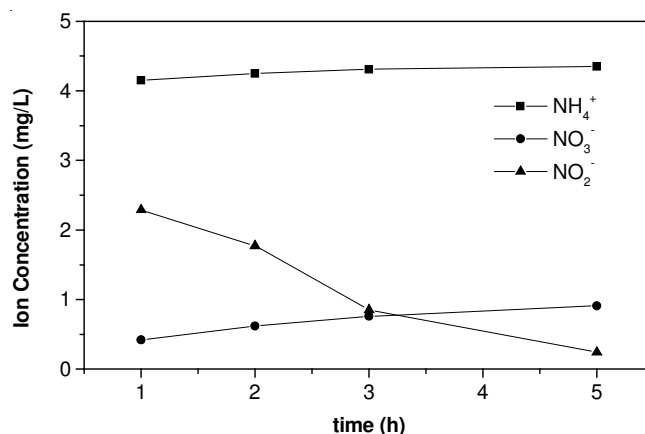


Fig. 6. Time course of inorganic ions produced during mineralization of 40 mg/L basic yellow 28 aqueous solution ( $[S_2O_8^{2-}]_0 = 9.87$  mM,  $[Fe^{2+}]_0 = 2$  mM,  $T = 65$  °C)

At the beginning of the oxidation process nitrite ion 511  
 concentration is seen to be more than the nitrate. However, 512  
 the nitrite ion concentration dropped quickly and reached 0.2 513  
 $mg\ L^{-1}$  after 5 h. The nitrate ions showed a slow rise during the 514  
 5 h up to  $1\ mg\ L^{-1}$  concentration. The nitrate concentration 515



516 remained stable at 4.2 mg L<sup>-1</sup> after 2 h. Hence, the sulfate ions  
517 formed from sources other than the dye molecule were not  
518 measured.

### 519 Conclusion

520 Degradation and mineralization of 40 mg L<sup>-1</sup> of the basic  
521 yellow 28 aqueous solution by the S<sub>2</sub>O<sub>8</sub><sup>2-</sup>/Fe<sup>2+</sup> system at pH  
522 3.5 was studied as a function oxidation time, temperature and  
523 initial concentration of Fe<sup>2+</sup> and S<sub>2</sub>O<sub>8</sub><sup>2-</sup>. The application of the  
524 Box-Benken design combined with the response surface  
525 modeling and optimization helped in attaining the optimal  
526 solution of reaching the maximum basic yellow 28 degradation  
527 in an aqueous solution by the S<sub>2</sub>O<sub>8</sub><sup>2-</sup>/Fe<sup>2+</sup> system. The optimum  
528 conditions were satisfied as 8 h treatment at 65 °C reaction  
529 temperature; 9.87 mM persulfate initial concentration and 1.95  
530 mM ferrous ion concentration; thereby realizing 93 % TOC  
531 removal per cent. It was demonstrated that the basic yellow  
532 28 structure is broken down into two main aromatic interme-  
533 diates early in the process. To reach a TOC removal percent of  
534 93 %, it was observed that the above mentioned aromatic struc-  
535 tures underwent a ring opening as well as the occurrence of  
536 smaller structures, such as organic carboxylic acids.

### ACKNOWLEDGEMENTS

537 The authors are grateful to the Mersin University Research  
538 Found (contract no: BAB-FEF KB (BG) 2010-4A) for the  
539 financial support and Mersin University Research and Appli-  
540 cation Center (MEITAM) for providing the facilities at the  
541 GC-MS and ion chromatography analysis.

### REFERENCES

- O.J. Hao, H. Kim and P.C. Chang, *Crit. Rev. Environ. Sci. Technol.*, **30**, 449 (2000).
- S.F. Li, *Bioresour. Technol.*, **101**, 2197 (2010).
- K.C. Huang, R.A. Couttenye and G.E. Hoag, *Chemosphere*, **49**, 413 (2002).
- C. Liang, C.J. Bruell, M.C. Marley and K.L. Sperry, *Chemosphere*, **55**, 1213 (2004).
- G.P. Anipsitakis and D.D. Dionysiou, *Appl. Catal. B*, **54**, 155 (2004).
- T.K. Lau, W. Chu and N.J.D. Graham, *Environ. Sci. Technol.*, **41**, 613 (2007).
- X.R. Xu and X.Z. Li, *Sep. Purif. Technol.*, **72**, 105 (2010).
- L. Ebersson, *Electron Transfer Reactions in Organic Chemistry*, Springer-Verlag, Berlin (1987).
- I.M. Kolthoff, A.I. Medalia and H.P. Raaen, *J. Am. Chem. Soc.*, **73**, 1733 (1951).
- C. Liang, Z.S. Wang and C.J. Bruell, *Chemosphere*, **66**, 106 (2007).
- I.H. Cho and K.D. Zoh, *Dyes Pigments*, **75**, 533 (2007).
- Y. Wu, S. Zhou, F. Qin, X. Ye and K. Zheng, *J. Hazard. Mater.*, **180**, 456 (2010).
- I. Arslan-Alaton, G. Tureli and T. Olmez-Hanci, *J. Photochem. Photobiol. A*, **202**, 142 (2009).
- S. Garcia-Segura, L.C. Almeida, N. Bocchi and E. Brillas, *J. Hazard. Mater.*, **194**, 109 (2011).
- A.R. Khataee, M. Zarei and S.K. Asl, *J. Electroanal. Chem.*, **648**, 143 (2010).
- I. Yahiaoui, F. Aissani-Benissad, F. Fourcade and A. Amrane, *Environ. Prog. Sustain. Energy*, **31**, 515 (2012).
- M.J. Lee, Y.S. Kim, C.K. Yoo, J.H. Song and S.J. Hwang, *Environ. Technol.*, **31**, 7 (2010).
- L. Lei, Q. Dai, M. Zhou and X. Zhang, *Chemosphere*, **68**, 1135 (2007).
- A. Kumar, B. Prasad and I.M. Mishra, *J. Hazard. Mater.*, **150**, 174 (2008).
- K.P. Singh, S. Gupta, A.K. Singh and S. Sinha, *J. Hazard. Mater.*, **186**, 1462 (2011).
- C.J. Liang, C.J. Bruell, M.C. Marley and K.L. Sperry, *Soil Sediment Contam.*, **12**, 207 (2003).
- K.C. Huang, Z. Zhao, G.E. Hoag, A. Dahmani and P.A. Block, *Chemosphere*, **61**, 551 (2005).
- R.H. Waldemer, P.G. Tratnyek, R.L. Johnson and J.T. Nurmi, *Environ. Sci. Technol.*, **41**, 1010 (2007).
- S.Y. Oh, H.W. Kim, J.M. Park, H.S. Park and C. Yoon, *J. Hazard. Mater.*, **168**, 346 (2009).
- S.X. Li, D. Wei, N.K. Mak, Z.W. Cai, X.R. Xu, H.B. Li and Y. Jiang, *J. Hazard. Mater.*, **164**, 26 (2009).
- P. Nfodzo and H. Choi, *Chem. Eng. J.*, **174**, 629 (2011).
- B. Jancic-Stojanovic, A. Malenovic, D. Ivanovic, T. Rakic and M. Medenica, *J. Chromatogr. A*, **1216**, 1263 (2009).
- M.A. Bezerra, R.E. Santelli, E.P. Oliveria, L.S. Villar and L.A. Escalera, *Talanta*, **76**, 965 (2008).
- R.H. Myers and D.C. Montgomery, *Response Surface Methodology: Process and Product Optimization using Designed Experiments*, John Wiley & Sons, USA, edn. 2 (2002).
- S. Hammami, N. Oturan, N. Bellakhal, M. Dachraoui and M.A. Oturan, *J. Electroanal. Chem.*, **610**, 75 (2007).
- S. Ghasempour, S.F. Torabi, S.O. Ranaei-Siadat, M. Jalali-Heravi, N. Ghaemi and K. Khajeh, *Environ. Sci. Technol.*, **41**, 7073 (2007).
- H.L. Liu and Y.R. Chiou, *Chem. Eng. J.*, **112**, 173 (2005).
- A.R. Khataee, *Environ. Technol.*, **31**, 73 (2010).
- M.J. Anderson and P.J. Whitcomb, *RSM Simplified, Optimizing Processes using Response Surface Methods for Design of Experiments*, CRC Press Taylor & Francis Group, New York (2005).
- W.J. Mcelroy and S.J. Waygood, *J. Chem. Soc. Faraday Trans.*, **86**, 2557 (1990).
- J.D. Laats and T.G. Le, *Environ. Sci. Technol.*, **39**, 1811 (2005).
- M.S. Tsao and W.K. Wilmarth, *J. Phys. Chem.*, **63**, 346 (1959).
- B. Gozmen, M. Turabik and A. Hesenov, *J. Hazard. Mater.*, **164**, 1487 (2009).
- E. Brillas, M.A. Banos and J.A. Garrido, *Electrochim. Acta*, **48**, 1697 (2003).
- Design-Expert Software version 8.00 User's Guide (2010).
- B. Neppolian, H. Jung, H. Choi, J.H. Lee and J.W. Kang, *Water Res.*, **36**, 4699 (2002).